

Geophysical Research Letters®

RESEARCH LETTER

10.1029/2023GL106944

Haiyuan Yang and Jinzhuo Cai contributed equally to this work.

Key Points:

- The East China Sea Kuroshio is intensifying while the Ryukyu Current is rapidly declining in a warming climate
- The change is mainly caused by enhanced stratification which induces uplift of current system and weaker topography-flow interaction

Supporting Information:

Supporting Information may be found in the online version of this article.

Correspondence to:

H. Yang,
yanghaiyuan@ouc.edu.cn






Citation:

Yang, H., Cai, J., Wu, L., Guo, H., Chen, Z., Jing, Z., & Gan, B. (2024). The intensifying East China Sea Kuroshio and disappearing Ryukyu Current in a warming climate. *Geophysical Research Letters*, 51, e2023GL106944. <https://doi.org/10.1029/2023GL106944>

Received 23 OCT 2023

Accepted 8 JUN 2024

The Intensifying East China Sea Kuroshio and Disappearing Ryukyu Current in a Warming Climate

Haiyuan Yang^{1,2} , Jinzhuo Cai¹, Lixin Wu^{1,2}, Haihong Guo² , Zhaohui Chen^{1,2} , Zhao Jing^{1,2} , and Bolan Gan^{1,2} 

¹Frontier Science Center for Deep Ocean Multispheres and Earth System (FDOMES)/Academy of the Future Ocean and Physical Oceanography Laboratory, Ocean University of China, Qingdao, China, ²Laoshan Laboratory, Qingdao, China

Abstract The East China Sea Kuroshio (ECS-Kuroshio) and the Ryukyu Current are the major poleward heat carriers in the North Pacific. Anomalous changes of ECS-Kuroshio and Ryukyu Current could exert substantial influence on the climate in mid-latitude regions. However, owing to limited observations and coarse resolution of climate models, how they might change under anthropogenic warming remains unknown. Here, we find an accelerating ECS-Kuroshio (1.5 Sv) and a decelerating (−2.2 Sv) Ryukyu Current using in-situ observation during 1958–2022, equivalent to 7% strengthening and 20% weakening in the 65 years. The trend is also simulated by four high-resolution climate models, with multi-model ensemble-mean acceleration (deceleration) of the ECS-Kuroshio (Ryukyu Current) of 1.2 ± 0.6 Sv (-6.2 ± 2.5 Sv) over 1950–2050. The weakening subtropical wind field reduces their summed transport. Enhanced stratification, which induces uplift of current system and weaker topography-flow interaction, leads to the intensifying ECS-Kuroshio and disappearing Ryukyu Current.

Plain Language Summary The East China Sea Kuroshio (ECS-Kuroshio) and the Ryukyu Current are the major components of western boundary current (WBC) system in the North Pacific. They transport large amount of heat poleward, maintaining the mid-latitude region warm and habitable. In this study, we find that in both observation and high-resolution numerical models, the ECS-Kuroshio is intensifying and the Ryukyu Current is rapidly declining. Particularly, in climate models, the Ryukyu Current is predicted to experience a 45% weakening during 1950–2050. Weakening wind field in the North Pacific tends to reduce the total transport of WBC system. The rapid weakening of the Ryukyu Current is credit to the enhanced stratification under global warming, which induces uplift of the Kuroshio east of Taiwan. Hence, less water will be blocked by bottom topography (Ilan Ridge) and bifurcates into the Ryukyu Current. Our finding highlights the needs for comprehensive studies on the local and climate effects of the evolution of the WBC system in the North Pacific.

1. Introduction

The Kuroshio stands as the primary ocean current along the western boundary of the North Pacific Ocean, facilitating the efficient exchange of mass and energy between tropical and mid-latitude regions (D. Hu et al., 2015; Imawaki et al., 2013; Qiu et al., 1991; F. Wang et al., 2023). Northeast of Taiwan, the Kuroshio Current interacts with the Ilan Ridge (24.5°N, 122°–124°E; averaging a depth of 600 m) and bifurcates into two branches (Thoppil et al., 2016; M. Wang et al., 2019; Figure 1a). The major branch flows over the Ilan Ridge into the East China Sea (ECS) and forms the ECS-Kuroshio. It meanders along the continental slopes of the ECS with a volume transport of around 24 Sv (1 Sv = 10^6 m³/s; Andres, Wimbush, et al., 2008; Liu et al., 2021). The other branch, the subsurface Ryukyu Current, travels along the eastern coast of the Ryukyu Islands with a transport ranging from 10 to 16 Sv (Ichikawa et al., 2004; You & Yoon, 2004; Zhao et al., 2020) and eventually merges with the ECS-Kuroshio at the Tokara Strait.

The anomalous changes in the ECS-Kuroshio and Ryukyu Current system (KRS) have a significant impact on mid-latitude regions. The intensification of the KRS enhances poleward heat transport (J. Cai et al., 2023; Omrani et al., 2019) and contributes to warming in the Kuroshio Extension region (Wu et al., 2012). The anomalously high sea surface temperature (SST) may increase the likelihood of marine heatwave formation (Holbrook et al., 2019), hinder the oceans' capacity to absorb anthropogenic carbon dioxide from the atmosphere (Bauer et al., 2013; W. J. Cai et al., 2006; DeVries, 2022), and promote the generation of more vigorous atmospheric storms (Hoskins & Valdes, 1990; Seo et al., 2023). Conversely, a weakening KRS could result in reduced heat transport, potentially alleviating downstream heat accumulation and reduce the risk of associated disasters.

© 2024. The Author(s).

This is an open access article under the terms of the [Creative Commons Attribution-NonCommercial-NoDerivs License](https://creativecommons.org/licenses/by/4.0/), which permits use and distribution in any medium, provided the original work is properly cited, the use is non-commercial and no modifications or adaptations are made.

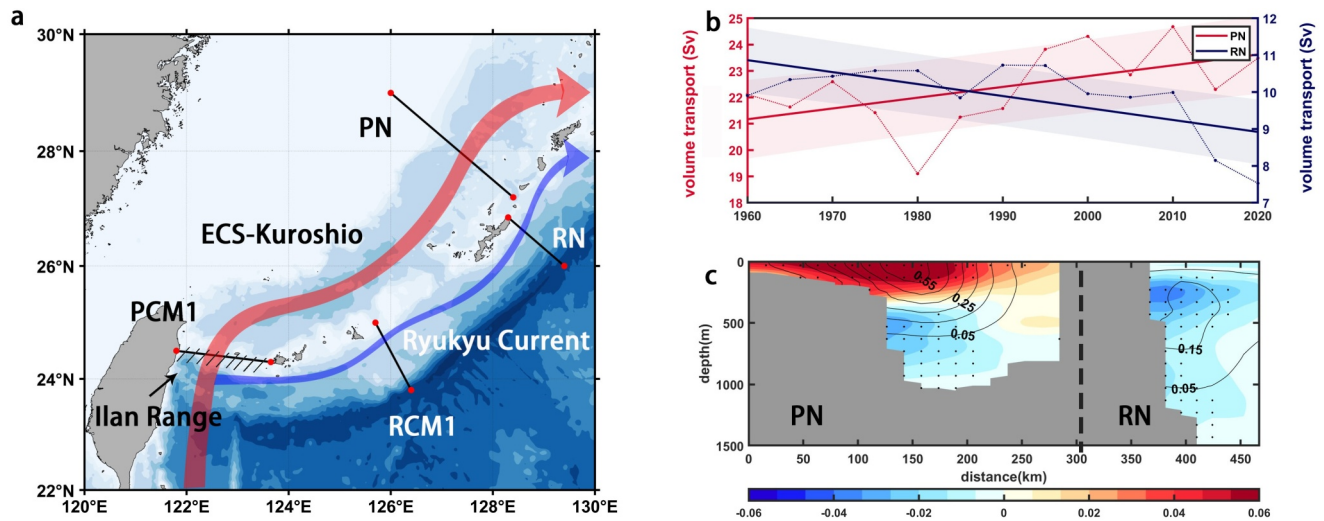


Figure 1. Observed intensifying ECS-Kuroshio and rapid-weakening Ryukyu Current. (a) Topography of East China Sea and Ryukyu Island Chain. Solid lines with red dots denote the locations of sections. (b) Transport in the upper-2,000 m across PN (red dots) and RN (blue dots) sections. Thick red (blue) line denotes linear fit of transport, while corresponding shading shows the 95% predict interval. Both trends are significant at 95% confidence level by Student's *t*-test. (c) Linear trend of geostrophic velocity (m/s/century) across PN and RN sections during 1958–2022. Positive (negative) values indicate acceleration (deceleration) of the current. The black dots represent the trends that are significant above the 95% confidence level by Student's *t*-test. The solid black contours are the time-mean geostrophic velocity.

In response to a warming climate, the western boundary current (WBC) system in the North Pacific has been observed to shift poleward (Yang et al., 2020), resulting in enhanced warming in the extension region (Wu et al., 2012). However, the debate continues regarding how the intensity of ECS-Kuroshio and the Ryukyu Current might change (J. Cai et al., 2023; Chen et al., 2019; Liu et al., 2021; Sen Gupta et al., 2021; Toda & Watanabe, 2020; Y. L. Wang & Wu, 2018; Wei et al., 2013; Wu et al., 2012; Yang et al., 2016). Existing observations on KRS mainly focused on ECS-Kuroshio (Andres, Wimbush, et al., 2008; Liu et al., 2021), while observations of the Ryukyu Current are still limited because of its subsurface feature. This has led to a gap between changes in WBC transport and the evolution of the wind field in the North Pacific over recent decades (Liu et al., 2022; Y. Zhang et al., 2020). Suffering from the coarse resolution, climate models also cannot fully reproduce the features of KRS (J. Cai et al., 2023; Sen Gupta et al., 2021). Consequently, understanding how the characteristics of the KRS might change, which is crucial for comprehending alterations in adjacent marginal seas/coastal areas and downstream mid-latitude regions, remains unknown. Here we show a weakening KRS with intensifying ECS-Kuroshio and rapid-weakening Ryukyu Current in observations, which is projected to persist in the future based on available high-resolution climate models.

2. Data and Methods

2.1. Data

To the northeast of Taiwan, the Kuroshio Current interacts with the Ilan Ridge and bifurcates into ECS-Kuroshio and Ryukyu Current (Figure 1a). To consolidate the evolution of these two currents, we initially utilize geostrophic velocity derived from the shipboard observations provided by Japan Meteorological Agency (JMA; Text S1 in Supporting Information S1). The product offers over 4×10^6 points of ocean temperature and salinity on isobaric surface with in 25° – 30° N, 125° – 130° E, covering PN (straight line connecting 29° N, 126° E and 27° N, 128.5° E) and RN (straight line connecting 26.8° N, 128.3° E and 26.2° N, 129.2° E) sections (Figure 1a). Commencing from 1958 and continuing to 2022, the data provide a valuable opportunity to study the long-term trend of KRS.

Apart from observational data, we also explore the velocity trends of the KRS from 1950 to 2050 using four available high-resolution climate models (HR models; see Table S1; refer to Text S2 in Supporting Information S1). These models boast a spatial resolution of 0.1° , enabling them to incorporate complex topography and accurately simulate the narrow WBC. Among the four HR models, three are obtained from the High-Resolution Model Intercomparison Project (HighResMIP; Haarsma et al., 2016), which are run under historical forcing from

1950 to 2014 and socioeconomic pathway 585 (SSP585) forcing from 2015 to 2050. Additionally, a high-resolution simulation based on the Community Earth System Model version 1.3 by the International Laboratory for High-Resolution Earth System Prediction (CESM-iHESP; Chang et al., 2020) is utilized, which uses historical forcing from 1950 to 2005 and representative concentration pathway 8.5 (RCP8.5) forcing from 2006 to 2050. In addition, we also performed model validation on these high-resolution models and found they reasonably simulate the intensity of ECS-Kuroshio, the Ryukyu Current as well as mesoscale activities. Please refer to Text S3 in Supporting Information S1 for more information.

2.2. Methods

To estimate geostrophic velocity, the in-situ temperature and salinity is first converted into potential density using seawater package. Then the upper-2,000 m PN section is gridded in the along-section and vertical directions with a horizontal (vertical) resolution of 14 km (20 m), respectively. Similarly, the resolution of grid for RN section is 12 km (20 m) in horizontal (vertical) direction. To ensure that each point on the spatial grids has enough observations, we divide the period of 1958–2022 into 13 periods. Thus, the temporal resolution of observation data is set to be 5 years. The potential density at each point of PN (RN) section is calculated as the average of all observations on the same depth level and period with horizontal distance to grid less than 14 km (12 km). Finally, thermal wind relation is applied to potential density to obtain the vertical gradient of horizontal geostrophic velocity. For more details of the data processing, please refer to Text S1 and Figure S1 in Supporting Information S1.

3. Enhanced ECS-Kuroshio and Disappearing Ryukyu Current Under Global Warming

Over the past 65 years, the transports of ECS-Kuroshio and the Ryukyu Current depict opposite trends. The ECS-Kuroshio transport across PN section increases from 22 Sv (1958–1962) to 23.5 Sv (2018–2022), indicating a 7% intensification. In contrast, the Ryukyu Current across RN section weakens by 20% with a linearly fitted reduction of 2.2 Sv over the past 65 years (Figure 1b), resulting in a 0.7-Sv-shrinking of KRS transport. The acceleration of the ECS-Kuroshio and deceleration of the Ryukyu Current are also evident in the vertical structure (Figure 1c). The Ryukyu Current exhibits deceleration from surface to 1,500 m, with a subsurface minimum value of -0.04 m/s/century near the core (300–400 m). In comparison, the ECS-Kuroshio shows an intensifying and uplift trend, with positive velocity trends (maximum reaches 0.07 m/s/century) on the surface and negative velocity trends (maximum reaches -0.03 m/s/century) below 400 m. Next, we will show that such trends are also robust in a century-long timescale in HR models.

Before using the HR models to explore the trends and the underlying mechanisms of the KRS, it is necessary to validate the robustness of the models. Further investigation shows that the HR models largely reproduces the observed KRS characteristics, including the ECS-Kuroshio with transport of 25 Sv across PN section and the 12 Sv Ryukyu Current with core locating at 500 m across RN section (Figures 2a and 2c), consisting well with observations and reanalysis data (Table S2 in Supporting Information S1). In addition to PN and RN, two additional sections, PCM1 and RCM1, are also involved to describe the upstream KRS (Johns et al., 2001; Zhao et al., 2020; location of the sections are shown in Figure 1a). It is found that the ECS-Kuroshio exhibits a 21 Sv transport across PCM1 section and the Ryukyu Current displays a 6 Sv transport across RCM1 section, both are consistent with observation/reanalysis values. Furthermore, the depth of the Ryukyu Current is roughly 500 m across both RCM1 and RN sections in the HR models, demonstrating similar values to observations and performing better than the reanalysis data. Moreover, we have also evaluated the models with horizontal resolutions ranging 0.25° – 1° in simulating KRS but found their failure in capturing the main current characteristics (Table S3 and Figure S2 in Supporting Information S1). Therefore, only HR models with horizontal resolutions of 0.1° are used in this study.

We compute the linear trend of velocity and transport across four sections (Figures 2a–2d; locations of PN, RN, PCM1 and RCM1 are shown in Figure 1a) in HR model simulations over the period of 1950–2050. The trends show weakening of Ryukyu Current and strengthening of ECS-Kuroshio in both the upstream and downstream (Figures 2a–2d). Although the strength may vary with models, the projected intensification of ECS-Kuroshio and decelerating Ryukyu Current are simulated in all models (Figures 2e and 2f). The magnitude of transport trends varies with locations. The changing rates of ECS-Kuroshio transport are 0.6 ± 0.5 Sv/century (0.6 denotes four-

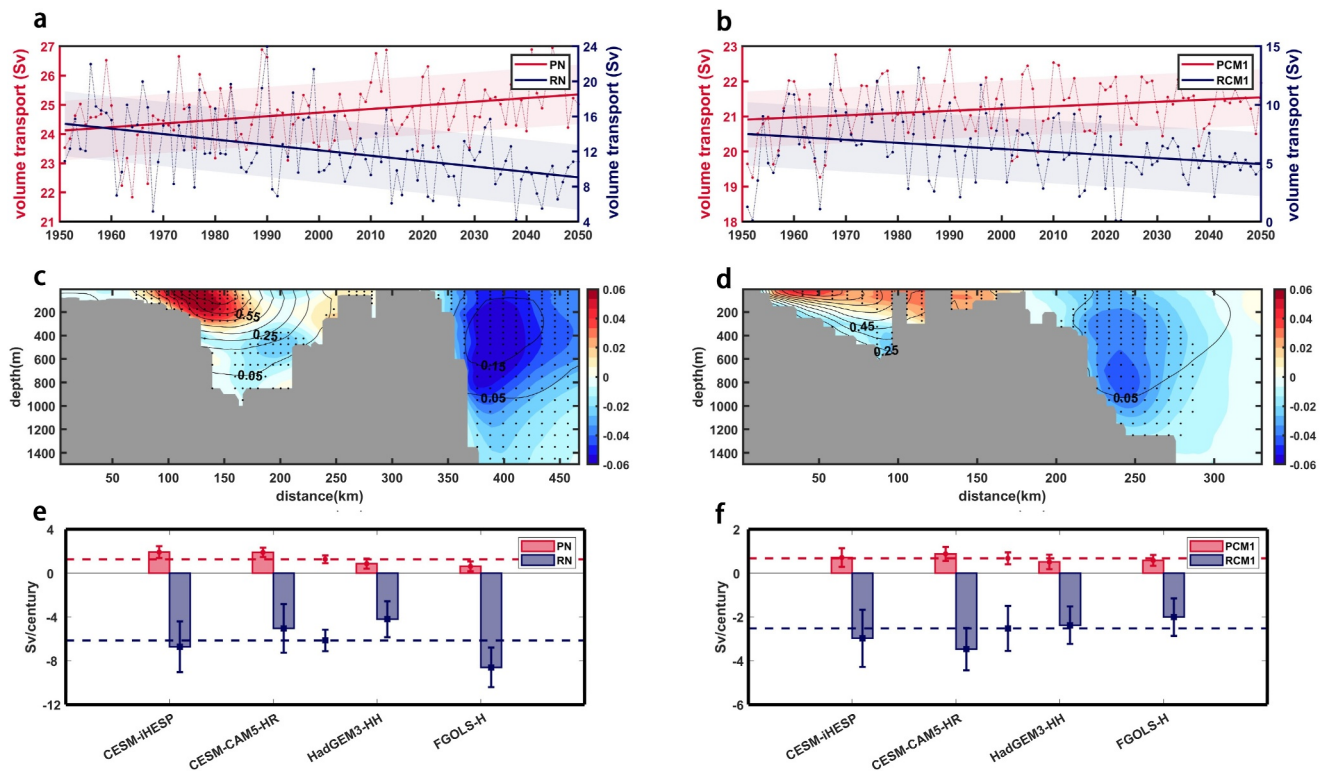


Figure 2. Simulated trend of ECS-Kuroshio and Ryukyu Current under global warming. (a) Timeseries of volume transport in upper 2,000 m across PN (red dots) and RN (blue dots) sections. Thick red (blue) line denotes linear fit of PN (RN) transport, while corresponding shading shows the 95% predict interval. Both trends are significant at 95% confidence level by Student's *t*-test. (c) Linear trend of velocity (m/s/century) across PN and RN sections during 1950–2050 in high resolution models. The black dots represent the trends that are statistically significant above the 95% confidence level by Student's *t*-test. The solid black contours are the time-mean velocity. (e) Volume transport trend of PN (red bars) and RN (blue bars) in individual models, corresponding error-bars display 95% confidence level by Student's *t*-test. Dashed lines and error-bars denote the ensemble mean trend at PN (red) and RN (blue) section and associated model spread defined as standard deviation. Panels (b, d, and f) are similar with panels (a, c, and e) but for PCM1 and RCM1.

model ensemble mean and ± 0.5 indicate inter-model spread) at PCM1 and 1.2 ± 0.6 Sv/century at PN, while the weakening rate of Ryukyu Current reaches -2.6 ± 0.3 Sv/century at RCM1 and -6.2 ± 2.5 Sv/century at RN. In both 24° and 28° N, KRS depicts a weakening trend which is dominated by the reduction of Ryukyu Current. Particularly, the Ryukyu Current is projected to be weakened by 34% at RCM1 and 45% at RN section till the middle of this century. Moreover, the changing rate of transports along 28° N is 2.5 times larger than that along 24° N. For the vertical structure, the uplift of ECS-Kuroshio and shrinking of Ryukyu Current between 0 and 1,500 m in observation (Figure 1c) are also revealed in model simulations (Figure 2c). The ECS-Kuroshio depicts a surface intensification in both PN and PCM1, while the Ryukyu Current decelerates from surface to bottom, with a max weakening rate near the current core.

4. Weaker Surface Wind and Enhanced Stratification in the North Pacific

Based on both observations and HR models, a scenario of a disappearing Ryukyu Current, which predominantly influences the transport change of the KRS, alongside an intensifying and uplifting ECS-Kuroshio, is suggested under global warming. Two potential processes that may drive the changes are subtropical wind field (Sen Gupta et al., 2021; Stommel, 1948; Sverdrup, 1947) and oceanic stratification (Pedlosky, 2013; Peng et al., 2022). The former directly affects the total volume transport of WBCs whereas the latter shapes their vertical structure. For instance, major WBCs' transport is associated with corresponding trends of basin-scale wind stress curl (J. Cai et al., 2023; Sen Gupta et al., 2021). Additionally, the enhanced vertical stratification intensifies the upper subtropical gyre, leading to a strengthening of WBCs in a warming climate (S. Hu et al., 2020; Peng et al., 2022). To explore the role of wind and stratification under global warming, we proceed to assess their changes in the climate models.

According to the wind-driven circulation theory, the energetic WBC is generated to dissipate the negative vorticity inserted by negative wind stress curl over subtropical ocean (Figure 3a; Pedlosky, 2013; Stommel, 1948; Sverdrup, 1947). In response to a warming climate, subtropical trade winds and westerlies are suggested to be weakened (Lu et al., 2007; Y. L. Wang & Wu, 2018; Y. Zhang et al., 2020), resulting from the decreasing meridional temperature gradient ascribed to the amplified Arctic warming (He et al., 2015; Xia et al., 2020). Therefore, the negative wind stress curl over the North Pacific depicts a positive trend under anthropogenic warming (Figure 3b; Text S4 in Supporting Information S1; Li et al., 2019; X. Zhang et al., 2014). Quantitatively, the strength of the zonal mean wind stress curl in 24°N (28°N) decreases by 7% (12%) from that of the climatology mean.

The vertical extent of ocean circulation system is regulated by ocean stratification (Guo et al., 2022), primarily determined by ocean temperature and salinity (Figures 3c–3e). Under global warming, the SST in North Pacific Ocean experiences a significant warming (X. M. Hu et al., 2021). In particular, the mean SST near the Ryukyu Island (23°N–33°N, 120°E–133°E) is suggested to increase by 2°C under climate change (Figure 3c). This temperature increase is restrained in the upper ocean and exhibits a decline with increasing depth, resulting in a stronger stratification of the ocean (Figure 3e; Capotondi et al., 2012). In addition to temperature, the subtropical North Pacific also experiences a basin-wide freshening with -0.05 psu/century due to increased precipitation (Sathyanarayanan et al., 2021). An enhanced freshening is observed in the vicinity of surface ECS with -0.2 psu/century (Figure 3d). However, this change in salinity has a secondary impact on oceanic stratification (Figure 3e). The spatial and vertical mean oceanic stratification near the Ryukyu Island (23°–33°N, 120°–133°E) is dominated by temperature changes and is projected to increase by $0.2 \times 10^{-5} \text{ s}^{-2}$ in upper 500 m, indicating a 17.2% intensification compared to the climatology mean. Affected by the stratification change, a more surface-intensified circulation is expected (Peng et al., 2022; Yamaguchi & Suga, 2019).

5. Response of KRS to Wind and Stratification Changes

According to Sverdrup theory, the volume transport of KRS is regulated by wind stress curl at the same latitude. Quantitatively, the strength of wind stress curl across 24°N decreases by 7% during 1950–2050, corresponding well with the -1.9 Sv change of volume transport of the KRS at the same latitude (Figure 4b). At 28°N, wind stress depicts a larger weakening rate of 12% (equal to a 4.8 Sv shrinking of current transport), which is also reflected on the more rapid volume transport decrease (-5.0 Sv; Figure 4a). As such, the total transport of KRS is regulated by weakening subtropical wind stress and is predicted to be continue in the near future. However, the opposite trends of the ECS-Kuroshio and Ryukyu Current cannot be explained simply by change of wind field.

A stronger stratification traps more energy in the upper ocean (Sun et al., 2013) inducing an up-lifted core of circulation system (Peng et al., 2022; Yamaguchi & Suga, 2019). In HR models, ECS-Kuroshio across PN (PCM1) section depicts a 0.02 (0.03) m/s/century intensifying rate at surface and a -0.01 (-0.01) m/s/century subsurface weakening rate (Figures 4c and 4d, red line). Despite the Ryukyu Current is projected to weaken from bottom to surface (Figures 4c and 4d, blue line), it is notable that the surface weakening rate is smaller than that around 500 m depth, which also indicates a moderate velocity center uplift. In addition to trapping energy in the upper layer directly, the stratification could also affect the flow-topography interaction in the Ilan Ridge, which is important in the generation of Ryukyu Current (Thoppil et al., 2016; M. Wang et al., 2019). A shallower Kuroshio east of Taiwan Island could decouple with bottom topography and less volume transport will be distributed into Ryukyu Current. Dynamically, the intensity of topography-flow interaction can be inferred by the bottom vertical velocity, which exhibits a dipole pattern across Ilan Ridge (Figure 4e; Text S5 in Supporting Information S1). The positive bottom vertical velocity indicates an up-hill movement, which compresses water column vertically and forms a clockwise bottom pressure torque, enabling the poleward current to turn east and originate the Ryukyu Current (Thoppil et al., 2016; M. Wang et al., 2019). Under global warming, the upward vertical velocity keeps weakening. Its trend depicts an opposite pattern compared to the climatology mean, indicating a weaker flow-topography interaction (Figure 4f). Correspondingly, the bottom horizontal velocity also depicts a weakening pattern, suggesting the Ryukyu Current is weakened from its origination point. In consequence, the Kuroshio tends to overlaps the Ilan Ridge rather than turns eastward, leading to the decline of the Ryukyu Current (Figure S5 in Supporting Information S1 and Figure 4f arrows).

To address the relation between “uplifting of Kuroshio” and the vertical structure of ECS-Kuroshio and Ryukyu Current, we add a section connecting 121.5°E, 23.3°N and 123.2°E, 22.8°N to describe the Kuroshio before

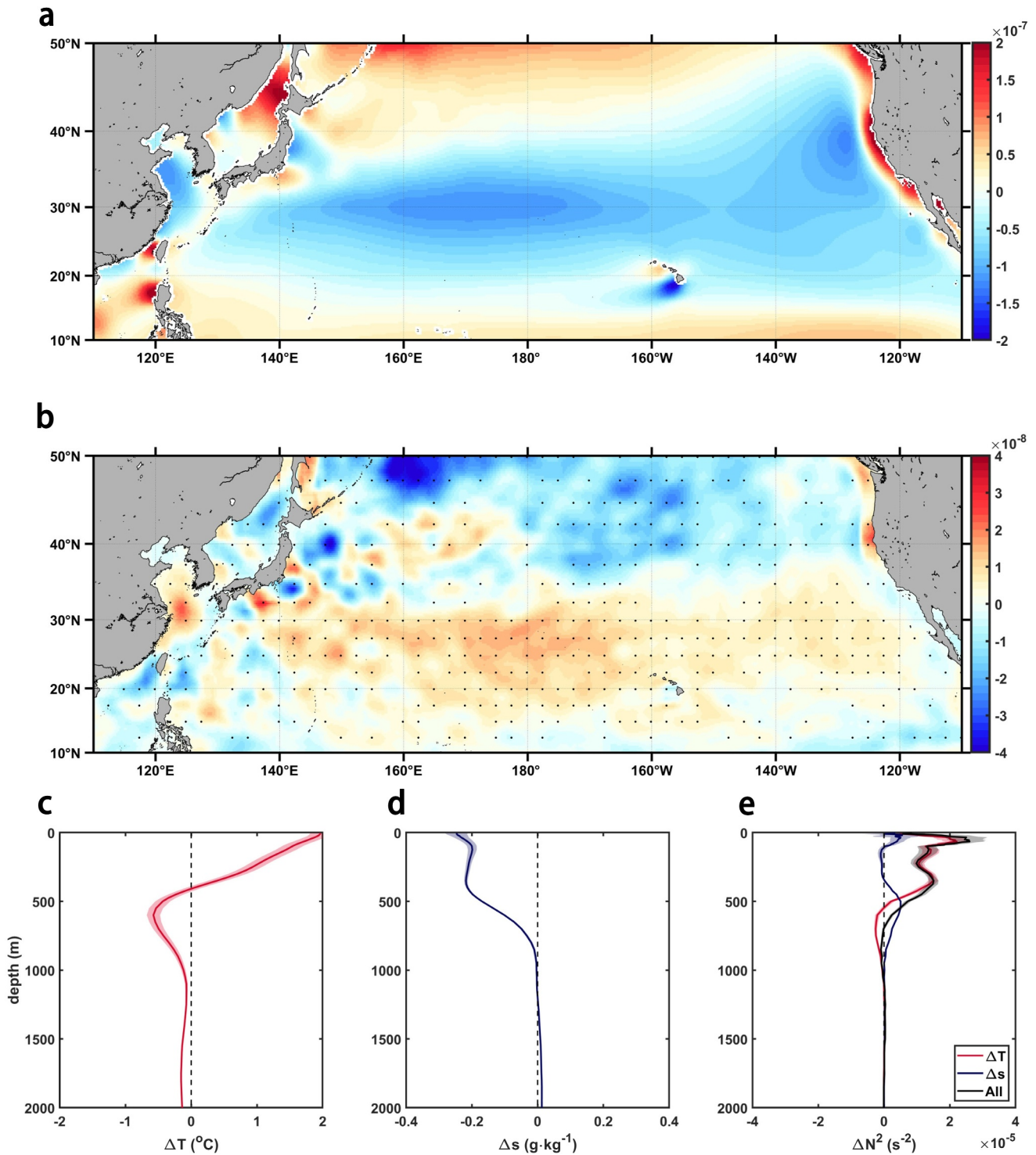


Figure 3. Changes in surface wind and stratification under global warming. (a and b) Time-mean wind stress curl during the historical period (a) and its change under global warming (b) in the North Pacific, based on the ensemble mean of 4 climate models. The black dots in b represent the values that are statistically significant above the 95% confidence level. (c and d) Changes of temperature and salinity during 1950–2050. (e) Black line and shading shows the change and 95% confidence interval of square of buoyancy frequency (N^2). Blue and red lines (shadings) are N^2 change induced by salinity and temperature.

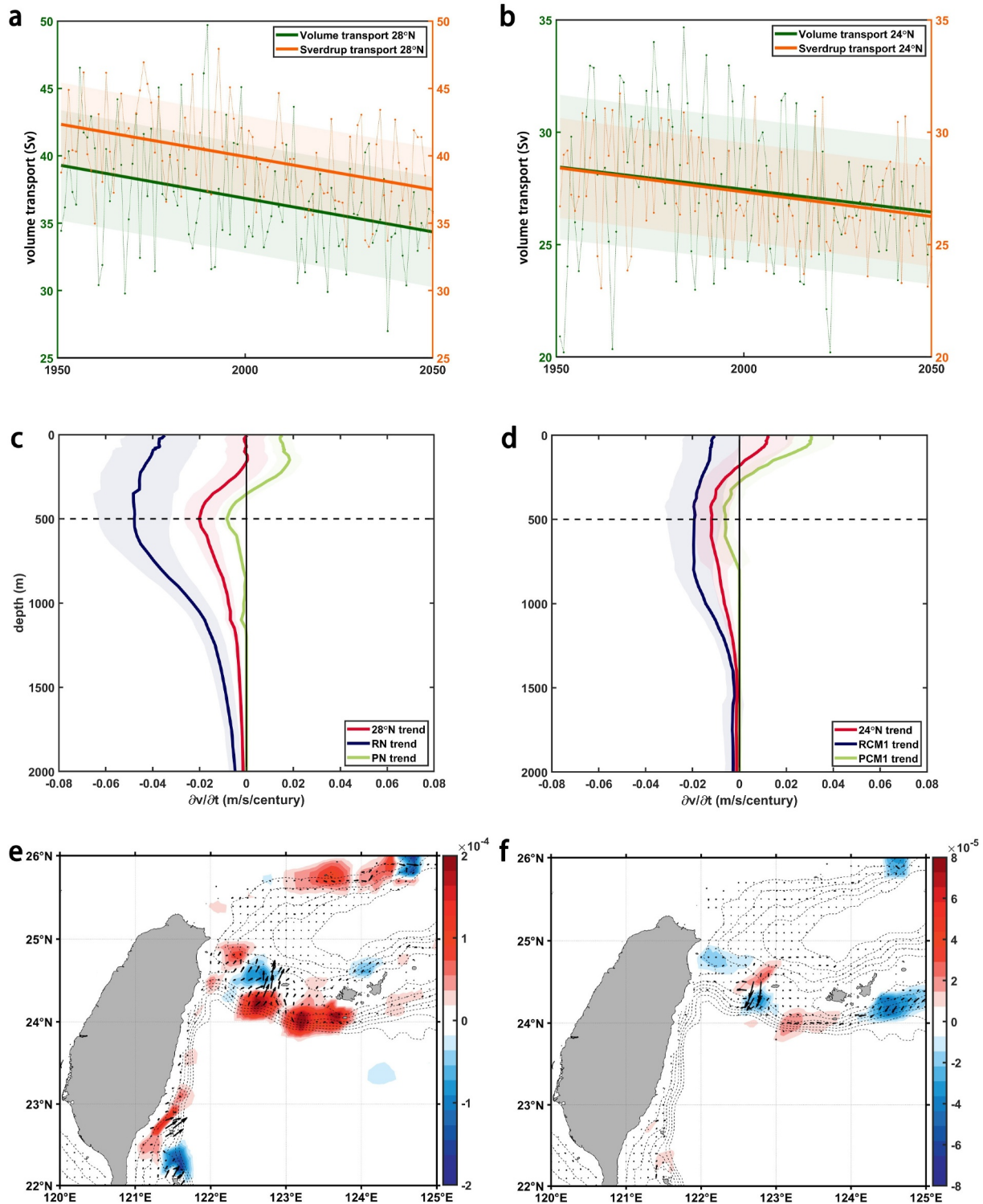


Figure 4. Model predicted KRS changes and bottom vertical velocity under global warming. (a) Changes in Sverdrup transport at 28°N (orange dots) and transport (above 2,000 m) across PN and RN sections (green dots), corresponding thick lines and shadings denote the linear fit value and the 95% predict interval. (b) Same as a but for PCM1 and RCM1 sections. (c) Red, blue and green lines indicate averaged velocity trend (m/s/century) at RN, PN sections and RN, PN as a whole. Corresponding shadings represent the 95% confidence intervals by Students' *t*-test. (d) Same as c but for RCM1 and PCM1 sections. (e) Climatology bottom vertical velocity (m/s; shading), thin dashed lines denote the bottom topography, while the arrows denote the bottom horizontal velocity. (f) Model simulated trend of bottom vertical velocity (m/s/century). The black dots in f represent the values that are significant above the 95% confidence level. The arrows denote the bottom horizontal velocity trend.

reaching the Ilan ridge. The stratification change (Figures S6a–S6c in Supporting Information S1) depicts large resemblance with that shown in Figures 3c–3e, indicating an enhanced stratification across the section. Moreover, we define the depth above which 80% of the total volume transport is achieved as the depth of Kuroshio. During 1950–2050, the depth of Kuroshio has a climatology value of 402 m and depicts a negative trend, decreasing from 450 to 350 m during the century, indicating the uplift of the Kuroshio happens east of Taiwan Island in HR models. Furthermore, the decreased depth consists well with the vertical structure in the trend of Ryukyu Current, whose weakening center locates between 300 and 600 m depth. Besides, Kuroshio depth is positively related to RN flux with a correlation coefficient of 0.64 (P -value <0.01 ; Figure S6d in Supporting Information S1), suggesting the uplift of Kuroshio favors a reduced Ryukyu Current. We also find the Kuroshio depth is negatively related to the PN volume transport with a correlation coefficient of -0.60 (P -value <0.01 ; Figure S6e in Supporting Information S1), further validating the uplifted Kuroshio is the main reason for the unbalanced distribution between Ryukyu Current and ECS-Kuroshio.

To further substantiate the importance of stratification and associated flow-topography interaction in affecting the origination and evolution of Ryukyu Current under global warming, two sets of idealized high-resolution experiments are designed based on the Massachusetts Institute of Technology general circulation model (MITgcm; Marshall et al., 1997; Text S6 in Supporting Information S1). The first set includes CTRL run and NOILAN run, both of them are forced with stratification before warming (temperature and salinity in climate models during 1950–1970; Figure S7a in Supporting Information S1). The topography in CTRL run is based on the reality in western Pacific with idealized Ryukyu Islands and Ilan Range (Figure S8a in Supporting Information S1), while the Ilan Range in NOILAN run is removed (Figure S8b in Supporting Information S1). In the second set of experiments (CTRL_WARMING run and NOILAN_WARMING run), model configurations are exactly same with CTRL run and NOILAN run, except for stratification is switched to the basin-wide averaged model simulated temperature and salinity during 2030–2050 (Figure S7b in Supporting Information S1), representing the scenario after warming. As such, we can estimate the role of enhanced stratification and associated flow-topography interaction in regulating the currents. In CTRL run (Figure S8c in Supporting Information S1), the ECS-Kuroshio flows along the continental slope with a maximum around 1.0 m/s, and the Ryukyu Current has a subsurface core with a maximum speed less than 0.2 m/s, in accord with in-situ observations (Imawaki et al., 2013). In the NOILAN run, the Ryukyu Current is weaker (Figure S8d in Supporting Information S1), suggesting that flow-topography interaction is important in the generation of Ryukyu Current. When the global warming signal associated with temperature change is added (Figures S8e and S8f in Supporting Information S1), the ECS-Kuroshio depicts a surface intensification in both CTRL_WARMING and NOILAN_WARMING run. The Ryukyu Current in CTRL_WARMING weakens by around 25% and is larger than that in NOILAN_WARMING (about 10%), indicating that the weaker flow-topography interaction enhances the unbalanced transport distribution between ECS-Kuroshio and Ryukyu Current.

This study emphasizes the impact of flow-topography interaction on the evolution of the Ryukyu Current under global warming. In addition, previous studies also suggest other mechanisms, including anticyclonic mesoscale variabilities (Liu et al., 2022; Nagai, 2023) and recirculation (Andres, Park, et al., 2008), in regulating the Ryukyu Current. However, a reduction of anticyclonic eddy activity between 24° and 26° N is inferred from sea level height trend (Figure S9 in Supporting Information S1) and an enhanced recirculation (Figure S10 in Supporting Information S1) during 1950–2050 is found based on high-resolution climate models, indicating they are not the causes for change of Ryukyu Current in the century-long timescale.

6. Discussion and Implication

Our finding of a weakening KRS with an intensifying ECS-Kuroshio and a disappearing Ryukyu Current under greenhouse warming is underpinned by weakened wind stress and intensified ocean stratification. The evolution of wind field leads to the reduction of the total transport of KRS. In comparison, the intensified ocean stratification induces uplift of currents and weaker flow-topography interaction, leading to the opposite change of ECS-Kuroshio and Ryukyu Current. This phenomenon is consistently simulated by all HR climate models, and the underlying mechanism is confirmed in idealized simulations.

Our discovery carries profound implications. Weakening of the KRS leads to a weaker poleward heat transport (Figures S11a and S11b; Text S7 in Supporting Information S1), which may mitigate the heat accumulation in the Kuroshio Extension region (Wu et al., 2012). However, climate models with coarse resolutions predict an

increasing heat transport (Figures S11c–S11f in Supporting Information S1), leaving large bias in assessing thermal evolution of downstream Kuroshio and correlated atmospheric evolutions (J. Cai et al., 2023; Yang et al., 2020). Therefore, our result highlights the needs for a comprehensive validation of the associated impacts and high-resolution monitoring systems in this region. In addition to the intensification, the ECS-Kuroshio is also found to experience a shoreward shift in the past decades (Guo et al., 2024). Actually, if we regard the KRS as a whole, the intensifying ECS-Kuroshio and disappearing Ryukyu Current also indicate a shoreward movement of this current system. As a result, more water from the tropical region will intrude into the ECS and trigger more marine heatwaves in the near future (Lee et al., 2023).

Data Availability Statement

The shipboard observation data used in this study can be acquired from J. Cai (2024). The source code of MITGCM model is obtained from Jean-Michel et al. (2023). The high-resolution models from HighresMIP are available from Roberts (2018), Bao and He (2019) and Hurrell et al. (2020). The CESM model source code and associated instructions are provided by Laoshan Laboratory and can be downloaded from RUO (2020).

Acknowledgments

This work was supported by Fundamental Research Funds for the Central Universities (202241006), the NSFC Major Research Plan on West-Pacific Earth System Multispheric Interactions (92258001), and National Natural Science Foundation of China (42176006 and 42225601). Computation for the work described in this paper was supported by the Marine Big Data Center of Institute for Advanced Ocean Study of Ocean University of China and Center for High Performance Computing and System Simulation of Laoshan Laboratory.

References

- Andres, M., Park, J. H., Wimbush, M., Zhu, X. H., Chang, K. I., & Ichikawa, H. (2008). Study of the Kuroshio/Ryukyu Current system based on satellite-altimeter and in situ measurements. *Journal of Oceanography*, 64(6), 937–950. <https://doi.org/10.1007/s10872-008-0077-2>
- Andres, M., Wimbush, M., Park, J. H., Chang, K. I., Lim, B. H., Watts, D. R., et al. (2008). Observations of Kuroshio flow variations in the East China Sea. *Journal of Geophysical Research*, 113(C5), C05013. <https://doi.org/10.1029/2007jc004200>
- Bao, Q., & He, B. (2019). CAS FGOALS-f3-H model output prepared for CMIP6 HighResMIP [Dataset]. *Earth System Grid Federation*. <https://doi.org/10.22033/ESGF/CMIP6.2041>
- Bauer, J. E., Cai, W. J., Raymond, P. A., Bianchi, T. S., Hopkinson, C. S., & Regnier, P. A. (2013). The changing carbon cycle of the coastal ocean. *Nature*, 504(7478), 61–70. <https://doi.org/10.1038/nature12857>
- Cai, J. (2024). JMA observation [Dataset]. *Zenodo*. <https://doi.org/10.5281/zenodo.10464820>
- Cai, J., Yang, H., Gan, B., Wang, H., Chen, Z., & Wu, L. (2023). Evolution of meridional heat transport by subtropical western boundary currents in a warming climate predicted by high-resolution models. *Journal of Climate*, 36(22), 8007–8025. <https://doi.org/10.1175/jcli-d-23-0100.1>
- Cai, W. J., Dai, M., & Wang, Y. (2006). Air-sea exchange of carbon dioxide in ocean margins: A province-based synthesis. *Geophysical Research Letters*, 33(12), L12603. <https://doi.org/10.1029/2006gl026219>
- Capotondi, A., Alexander, M. A., Bond, N. A., Curchitser, E. N., & Scott, J. D. (2012). Enhanced upper ocean stratification with climate change in the CMIP3 models. *Journal of Geophysical Research*, 117(C4), C04031. <https://doi.org/10.1029/2011jc007409>
- Chang, P., Zhang, S., Danabasoglu, G., Yeager, S. G., Fu, H., Wang, H., et al. (2020). An unprecedented set of high-resolution earth system simulations for understanding multiscale interactions in climate variability and change. *Journal of Advances in Modeling Earth Systems*, 12(12), e2020MS002298. <https://doi.org/10.1029/2020ms002298>
- Chen, C., Wang, G., Xie, S. P., & Liu, W. (2019). Why does global warming weaken the Gulf Stream but intensify the Kuroshio? *Journal of Climate*, 32(21), 7437–7451. <https://doi.org/10.1175/jcli-d-18-0895.1>
- DeVries, T. (2022). Atmospheric CO₂ and sea surface temperature variability cannot explain recent decadal variability of the ocean CO₂ sink. *Geophysical Research Letters*, 49(7), e2021GL096018. <https://doi.org/10.1029/2021gl096018>
- Guo, H., Cai, J., Yang, H., & Chen, Z. (2024). Observations reveal onshore acceleration and offshore deceleration of the Kuroshio Current in the East China Sea over the past three decades. *Environmental Research Letters*, 19(2), 024020. <https://doi.org/10.1088/1748-9326/ad1d3b>
- Guo, H., Spall, M. A., Pedlosky, J., & Chen, Z. (2022). A three-dimensional inertial model for coastal upwelling along western boundaries. *Journal of Physical Oceanography*, 52(10), 2431–2444. <https://doi.org/10.1175/jpo-d-22-0024.1>
- Haarsma, R. J., Roberts, M. J., Vidale, P. L., Senior, C. A., Bellucci, A., Bao, Q., et al. (2016). High Resolution Model Intercomparison Project (HighResMIP v1. 0) for CMIP6. *Geoscientific Model Development*, 9(11), 4185–4208. <https://doi.org/10.5194/gmd-9-4185-2016>
- He, C., Zhou, T., Lin, A., Wu, B., Gu, D., Li, C., & Zheng, B. (2015). Enhanced or weakened western North Pacific subtropical high under global warming? *Scientific Reports*, 5(1), 16771. <https://doi.org/10.1038/srep16771>
- Holbrook, N. J., Scannell, H. A., Sen Gupta, A., Benthuyssen, J. A., Feng, M., Oliver, E. C., et al. (2019). A global assessment of marine heatwaves and their drivers. *Nature Communications*, 10(1), 2624. <https://doi.org/10.1038/s41467-019-10206-z>
- Hoskins, B. J., & Valdes, P. J. (1990). On the existence of storm-tracks. *Journal of the Atmospheric Sciences*, 47(15), 1854–1864. [https://doi.org/10.1175/1520-0469\(1990\)047<1854:oteost>2.0.co;2](https://doi.org/10.1175/1520-0469(1990)047<1854:oteost>2.0.co;2)
- Hu, D., Wu, L., Cai, W., Gupta, A. S., Ganachaud, A., Qiu, B., et al. (2015). Pacific western boundary currents and their roles in climate. *Nature*, 522(7556), 299–308. <https://doi.org/10.1038/nature14504>
- Hu, S., Sprintall, J., Guan, C., McPhaden, M. J., Wang, F., Hu, D., & Cai, W. (2020). Deep-reaching acceleration of global mean ocean circulation over the past two decades. *Science Advances*, 6(6), eaax7727. <https://doi.org/10.1126/sciadv.aax7727>
- Hu, X. M., Ma, J. R., Ying, J., Cai, M., & Kong, Y. Q. (2021). Inferring future warming in the Arctic from the observed global warming trend and CMIP6 simulations. *Advances in Climate Change Research*, 12(4), 499–507. <https://doi.org/10.1016/j.accr.2021.04.002>
- Hurrell, J., Marika, H., Peter, G., Steven, G., Jennifer, K., Paul, K., et al. (2020). NCAR CESM1-CAM5-SE-HR model output prepared for CMIP6 HighResMIP [Dataset]. *Earth System Grid Federation*. <https://doi.org/10.22033/ESGF/CMIP6.14220>
- Ichikawa, H., Nakamura, H., Nishina, A., & Higashi, M. (2004). Variability of northeastward current southeast of northern Ryukyu Islands. *Journal of Oceanography*, 60(2), 351–363. <https://doi.org/10.1023/b:joce.0000038341.27622.73>
- Imawaki, S., Bower, A. S., Beal, L., & Qiu, B. (2013). Western boundary currents. In *International geophysics* (Vol. 103, pp. 305–338). Academic Press. <https://doi.org/10.1016/b978-0-12-391851-2.00013-1>
- Jean-Michel, C., Heimbach, P., Losch, M., Gael, F., Alistair, A., Dimitris, M., et al. (2023). MITgcm/MITgcm: Ckeckpoint68r [Software]. *Zenodo*. <https://doi.org/10.5281/zenodo.8208482>

- Johns, W. E., Lee, T. N., Zhang, D., Zantopp, R., Liu, C. T., & Yang, Y. (2001). The Kuroshio east of Taiwan: Moored transport observations from the WOCE PCM-1 array. *Journal of Physical Oceanography*, *31*(4), 1031–1053. [https://doi.org/10.1175/1520-0485\(2001\)031<1031:tkoetm>2.0.co;2](https://doi.org/10.1175/1520-0485(2001)031<1031:tkoetm>2.0.co;2)
- Lee, S., Park, M. S., Kwon, M., Park, Y. G., Kim, Y. H., & Choi, N. (2023). Rapidly changing East Asian marine heatwaves under a warming climate. *Journal of Geophysical Research: Oceans*, *128*(6), e2023JC019761. <https://doi.org/10.1029/2023jc019761>
- Li, Q., Luo, Y., & Liu, F. (2019). Response of the subtropical gyre circulation in the North Pacific Ocean to CO₂ quadrupling. *Atmosphere-Ocean*, *57*(4), 307–317. <https://doi.org/10.1080/07055900.2019.1666701>
- Liu, Z., Gan, J., Hu, J., Wu, H., Cai, Z., & Deng, Y. (2021). Progress of studies on circulation dynamics in the East China Sea: The Kuroshio exchanges with the shelf currents. *Frontiers in Marine Science*, *8*, 620910. <https://doi.org/10.3389/fmars.2021.620910>
- Liu, Z. J., Zhu, X. H., Nakamura, H., Wang, M., Nishina, A., Qiao, Y. X., & Zhu, Z. N. (2022). Response of the Ryukyu Current to climate change during 1993–2018: Is there a robust trend? *Journal of Geophysical Research: Oceans*, *127*(12), e2022JC018957. <https://doi.org/10.1029/2022jc018957>
- Lu, J., Vecchi, G. A., & Reichler, T. (2007). Expansion of the Hadley cell under global warming. *Geophysical Research Letters*, *34*(6), L06805. <https://doi.org/10.1029/2006gl028443>
- Marshall, J., Hill, C., Perelman, L., & Adcroft, A. (1997). Hydrostatic, quasi-hydrostatic, and nonhydrostatic ocean modeling. *Journal of Geophysical Research*, *102*(C3), 5733–5752. <https://doi.org/10.1029/96jc02776>
- Nagai, T. (2023). Weakened Kuroshio slows down the Ryukyu Current. Retrieved from <https://eos.org/editor-highlights/weakened-kuroshio-slows-down-the-ryukyu-current>
- Omrani, N. E., Ogawa, F., Nakamura, H., Keenlyside, N., Lubis, S. W., & Matthes, K. (2019). Key role of the ocean western boundary currents in shaping the Northern Hemisphere climate. *Scientific Reports*, *9*(1), 3014. <https://doi.org/10.1038/s41598-019-39392-y>
- Pedlosky, J. (2013). *Geophysical fluid dynamics*. Springer Science & Business Media.
- Peng, Q., Xie, S. P., Wang, D., Huang, R. X., Chen, G., Shu, Y., et al. (2022). Surface warming-induced global acceleration of upper ocean currents. *Science Advances*, *8*(16), eabj8394. <https://doi.org/10.1126/sciadv.abj8394>
- Qiu, B., Kelly, K. A., & Joyce, T. M. (1991). Mean flow and variability in the Kuroshio Extension from Geosat altimetry data. *Journal of Geophysical Research*, *96*(C10), 18491–18507. <https://doi.org/10.1029/91jc01834>
- Roberts, M. (2018). MOHC HadGEM3-GC31-HH model output prepared for CMIP6 HighResMIP [Dataset]. *Earth System Grid Federation*. <https://doi.org/10.22033/ESGF/CMIP6.445>
- RUO. (2020). lgan/cesm_sw_1.0.1: Some efforts on refactoring and optimizing the Community Earth System Model (CESM1.3.1) on the Sunway TaihuLight supercomputer (cesm_sw_1.0.1) [Software]. *Zenodo*. <https://doi.org/10.5281/zenodo.3637771>
- Sathyanarayanan, A., Köhl, A., & Stammer, D. (2021). Ocean salinity changes in the global ocean under global warming conditions. Part I: Mechanisms in a strong warming scenario. *Journal of Climate*, *34*(20), 8219–8236.
- Sen Gupta, A., Stella, A., Pontes, G. M., Taschetto, A. S., Vergés, A., & Rossi, V. (2021). Future changes to the upper ocean Western Boundary Currents across two generations of climate models. *Scientific Reports*, *11*(1), 9538. <https://doi.org/10.1038/s41598-021-88934-w>
- Seo, H., O'Neill, L. W., Bourassa, M. A., Czaja, A., Drushka, K., Edson, J. B., et al. (2023). Ocean mesoscale and frontal-scale ocean-atmosphere interactions and influence on large-scale climate: A review. *Journal of Climate*, *36*(7), 1981–2013. <https://doi.org/10.1175/jcli-d-21-0982.1>
- Stommel, H. (1948). The westward intensification of wind-driven ocean currents. *Eos, Transactions American Geophysical Union*, *29*(2), 202–206.
- Sun, S., Wu, L., & Qiu, B. (2013). Response of the inertial recirculation to intensified stratification in a two-layer quasigeostrophic ocean circulation model. *Journal of Physical Oceanography*, *43*(7), 1254–1269. <https://doi.org/10.1175/jpo-d-12-0111.1>
- Sverdrup, H. U. (1947). Wind-driven currents in a baroclinic ocean; with application to the equatorial currents of the eastern Pacific. *Proceedings of the National Academy of Sciences*, *33*(11), 318–326. <https://doi.org/10.1073/pnas.33.11.318>
- Thoppil, P. G., Metzger, E. J., Hurlburt, H. E., Smedstad, O. M., & Ichikawa, H. (2016). The current system east of the Ryukyu Islands as revealed by a global ocean reanalysis. *Progress in Oceanography*, *141*, 239–258. <https://doi.org/10.1016/j.pocean.2015.12.013>
- Toda, M., & Watanabe, M. (2020). Mechanisms of enhanced ocean surface warming in the Kuroshio region for 1951–2010. *Climate Dynamics*, *54*(9–10), 4129–4145. <https://doi.org/10.1007/s00382-020-05221-6>
- Wang, F., Li, X., Tang, X., Sun, X., Zhang, J., Yang, D., et al. (2023). The seas around China in a warming climate. *Nature Reviews Earth & Environment*, *4*(8), 535–551. <https://doi.org/10.1038/s43017-023-00453-6>
- Wang, M., Liu, Z., Zhu, X., Yan, X., Zhang, Z., & Zhao, R. (2019). Origin and formation of the Ryukyu Current revealed by HYCOM reanalysis. *Acta Oceanologica Sinica*, *38*(11), 1–10. <https://doi.org/10.1007/s13131-018-1329-7>
- Wang, Y. L., & Wu, C. R. (2018). Discordant multi-decadal trend in the intensity of the Kuroshio along its path during 1993–2013. *Scientific Reports*, *8*(1), 14633. <https://doi.org/10.1038/s41598-018-32843-y>
- Wei, Y., Huang, D., & Zhu, X. H. (2013). Interannual to decadal variability of the Kuroshio Current in the East China Sea from 1955 to 2010 as indicated by in-situ hydrographic data. *Journal of Oceanography*, *69*(5), 571–589. <https://doi.org/10.1007/s10872-013-0193-5>
- Wu, L., Cai, W., Zhang, L., Nakamura, H., Timmermann, A., Joyce, T., et al. (2012). Enhanced warming over the global subtropical western boundary currents. *Nature Climate Change*, *2*(3), 161–166. <https://doi.org/10.1038/nclimate1353>
- Xia, Y., Hu, Y., & Liu, J. (2020). Comparison of trends in the Hadley circulation between CMIP6 and CMIP5. *Science Bulletin*, *65*(19), 1667–1674. <https://doi.org/10.1016/j.scib.2020.06.011>
- Yamaguchi, R., & Suga, T. (2019). Trend and variability in global upper-ocean stratification since the 1960s. *Journal of Geophysical Research: Oceans*, *124*(12), 8933–8948. <https://doi.org/10.1029/2019jc015439>
- Yang, H., Lohmann, G., Krebs-Kanzow, U., Ionita, M., Shi, X., Sidorenko, D., et al. (2020). Poleward shift of the major ocean gyres detected in a warming climate. *Geophysical Research Letters*, *47*(5), e2019GL085868. <https://doi.org/10.1029/2019gl085868>
- Yang, H., Lohmann, G., Wei, W., Dima, M., Ionita, M., & Liu, J. (2016). Intensification and poleward shift of subtropical western boundary currents in a warming climate. *Journal of Geophysical Research: Oceans*, *121*(7), 4928–4945. <https://doi.org/10.1002/2015jc011513>
- You, S. H., & Yoon, J. H. (2004). Modeling of the Ryukyu Current along the Pacific side of the Ryukyu Islands. *Pacific Oceanography*, *2*, 44–51.
- Zhang, X., Church, J. A., Platten, S. M., & Monselesan, D. (2014). Projection of subtropical gyre circulation and associated sea level changes in the Pacific based on CMIP3 climate models. *Climate Dynamics*, *43*(1–2), 131–144. <https://doi.org/10.1007/s00382-013-1902-x>
- Zhang, Y., Zhang, Z., Chen, D., Qiu, B., & Wang, W. (2020). Strengthening of the Kuroshio Current by intensifying tropical cyclones. *Science*, *368*(6494), 988–993. <https://doi.org/10.1126/science.aax5758>
- Zhao, R., Nakamura, H., Zhu, X. H., Park, J. H., Nishina, A., Zhang, C., et al. (2020). Tempo-spatial variations of the Ryukyu Current southeast of Miyakojima Island determined from mooring observations. *Scientific Reports*, *10*(1), 6656. <https://doi.org/10.1038/s41598-020-63836-5>